Interface focus

J. R. Soc. Interface (2010) **7**, S295–S306
doi:10.1098/rsif.2010.0107.focus
Published online 31 March 2010

Review

Insights into the mechanisms of myosin and kinesin molecular motors from the single-molecule unbinding force measurements

Sergey V. Mikhailenko[1], Yusuke Oguchi[1] and Shin'ichi Ishiwata[1,2,3,*]

[1]*Department of Physics, Faculty of Science and Engineering, and* [2]*Advanced Research Institute for Science and Engineering, Waseda University, Tokyo 169-8555, Japan*
[3]*Waseda Bioscience Research Institute in Singapore (WABIOS), Singapore 138667, Republic of Singapore*

In cells, ATP (adenosine triphosphate)-driven motor proteins, both cytoskeletal and nucleic acid-based, operate on their corresponding 'tracks', that is, actin, microtubules or nucleic acids, by converting the chemical energy of ATP hydrolysis into mechanical work. During each mechanochemical cycle, a motor proceeds via several nucleotide states, characterized by different affinities for the 'track' filament and different nucleotide (ATP or ADP) binding kinetics, which is crucial for a motor to efficiently perform its cellular functions. The measurements of the rupture force between the motor and the track by applying external loads to the individual motor–substrate bonds in various nucleotide states have proved to be an important tool to obtain valuable insights into the mechanism of the motors' performance. We review the application of this technique to various linear molecular motors, both processive and non-processive, giving special attention to the importance of the experimental geometry.

Keywords: single molecules; optical tweezers; molecular motors; unbinding force; myosin; kinesin

1. INTRODUCTION

Within less than two decades after their appearance, the single-molecule measurements became routinely recognized as an invaluable tool to study various phenomena in biological systems. The speed at which the experimental techniques in this field have been developing is fascinating. The measurements tackling individual molecules and therefore not requiring the averaging of the experimental parameters over myriads of them have allowed researchers to directly observe the previously invisible processes (for review, Deniz *et al.* 2008).

In this review we will limit ourselves to the developments in probing the interaction between various molecular motors and their 'tracks'. As was noted more than 2000 years ago by Aristotle, 'Life is motion', and now we know that all kinds of movement in living organisms are borne by the molecular motors, which play key roles in virtually all cellular processes. Here, we almost exclusively discuss the cytoskeletal motor proteins, myosins and kinesins, which operate on their respective cytoskeleton filaments, actin and microtubules. Both myosins and kinesins are the adenosine triphosphate (ATP)-driven motors, which are able to bind and hydrolyse ATP to adenosine diphosphate (ADP) and a phosphate and convert the liberated chemical energy into mechanical work. During the hydrolysis process, the motor molecule proceeds via several nucleotide states, characterized by different affinities for the 'track' filament and different nucleotide binding kinetics, which is crucial for kinesins and myosins to efficiently perform their cellular functions. These characteristics differ between various myosin or kinesin classes, implying that each class is specially tuned for its particular cellular role. While performing their cellular tasks, the motor proteins generate force and sense the force, either from outside or that exerted by other molecules. Load significantly affects the motors' performance; it is thought that load may even control the cellular role of a motor, such as in the case of myosin VI, which is proposed to be able to switch between its roles of an oppositely directed vesicle

*Author for correspondence (ishiwata@waseda.jp).

One contribution to a Theme Supplement 'Mechanobiology'.

Received 25 February 2010
Accepted 12 March 2010

transporter and an anchor, by sensing the external load (Altman *et al.* 2004).

Therefore, the study of the molecular motors requires the ability to apply load to them and test their response. One of the most useful features of the single-molecule measurements is the unprecedented ability to exert forces on the molecules under scrutiny, and do it with great control and precision, which makes the single-molecule experiments an extremely powerful tool to probe the intracellular performance of various molecular motors. We will review here the unbinding force measurements on both the non-processive motors, such as a molecule of the muscle, myosin I and the processive motors, such as kinesin or myosins V and VI, which are able to repeat many ATPase cycles and travel long distances without dissociating from their 'tracks'.

2. UNBINDING FORCE MEASUREMENTS

2.1. Measuring the rupture force of the muscle myosin–actin bond

The theoretical framework for measurements of the force required to rupture intramolecular bonds (Bell 1978) had to wait for nearly 20 years before its suitability for the single motor–track interactions was tested. It was not until after the optical tweezers technique (Ashkin *et al.* 1986) had swiftly burst into the field of molecular motors (Svoboda *et al.* 1993; Finer *et al.* 1994; Molloy *et al.* 1995), following the discovery of an efficient way to visualize actin filaments using the fluorescent derivative of phalloidin (Yanagida *et al.* 1984), that it became experimentally possible to apply and measure forces which break individual actin–myosin bonds (Nishizaka *et al.* 1995). In this pioneering work, the force that ruptures a bond between actin and a single motor molecule of muscle, myosin II, was measured in the absence of ATP (that is, in the nucleotide-free, or rigour, state of the motor) by pulling an actin filament with optical tweezers (figure 1*a*). This was achieved by trapping the bead coated with gelsolin, a barbed end capping protein, with optical tweezers and attaching it to the barbed end of actin. The optical trap was then displaced in the direction parallel to the glass surface, on which double-headed proteolytic fragments of myosin, heavy meromyosin (HMM) molecules, were sparsely distributed. The stage displacement imposed a gradually increasing load on the bond between the actin filament and the nearest to the trap HMM molecule, until the bond ruptured (figure 1*b*,*c*). The measured average unbinding force, 9.2 ± 4.4 pN (figure 1*d*), was found to be only a few times larger than the force which a single myosin II molecule can generate during power stroke (Finer *et al.* 1994; Ishijima *et al.* 1994; Miyata *et al.* 1995), but much smaller than other measured intermolecular forces (such as, for example, 110 pN for actin–actin (Kishino & Yanagida 1988) or 160 pN for avidin–biotin (Florin *et al.* 1994) interaction). The unbinding events were observed repeatedly for the same myosin molecule (figure 1*a*,*e*), indicating that the forced rupture of an actomyosin bond does not lead to the denaturation of a myosin molecule. This study also found that an approximately 10 pN force accelerates the rate of myosin unbinding from actin in the absence of nucleotides by a factor of 10^2–10^3, decreasing the lifetime of a rigour bond from 10^2–10^3 s to approximately 1 s. From the theoretical predictions (Bell 1978; Erickson 1994), such acceleration corresponds to a relatively large interaction distance of approximately 2–3 nm [$(\ln(10^2$–$10^3))k_{\mathrm{B}}\mathrm{T}/10$ pN]. This was suggested to be the characteristic feature of a motor–track interaction, which was later confirmed by the measurements with other motors, such as kinesin (Uemura *et al.* 2002; Kawaguchi *et al.* 2003) and myosins V and VI (Oguchi *et al.* 2008; Gebhardt *et al.* 2010).

A more accurate determination of the load-dependent parameters of the actin–myosin binding required the modification of the experimental set-up (Nishizaka *et al.* 2000). In this study the same experimental geometry was used; however, force was applied to single actomyosin bonds by displacing the substage in a stepwise manner (less than or equal to 40 nm steps, trap stiffness 0.1–0.3 pN nm^{-1}; figure 1*f*). This method allowed for the precise determination of the imposed load from the displacement of a bead within the x–y plane (however, the contribution of the vertical component of load was not considered in this study). It was found that for single-headed proteolytic fragments of myosin, subfragment-1 (S1) molecules, the relationship between the lifetime (τ) of the actomyosin bond and the imposed load (F) could be expressed as $\tau(F) = \tau(0)\exp(-Fd/k_{\mathrm{B}}\mathrm{T})$, where $\tau(0)$ is the bond lifetime under no load, determined to be 67 s, and d, the characteristic distance of the interaction, was 2.4 nm (figure 1*g*). The same relationship for the double-headed HMM was expressed by the sum of the two exponentials, yielding two sets of $\tau(0)$ and d, being equal to 62 s and 2.7 nm (fast component) and 950 s and 1.4 nm (slow component). The parameters of the fast component coincided with those for S1, indicating that the fast and the slow components corresponded to the single-headed and the double-headed binding, respectively. The unbinding force is not an absolute value and depends on the loading rate, such that the higher loading rates result in the larger unbinding forces.

In another work, atomic force microscopy (AFM) was used to measure the forces that rupture single actomyosin bonds in the nucleotide-free state (Nakajima *et al.* 1997). A probe tip, to which single molecules of HMM were attached, scanned over an actin filament in a stepwise manner (repetitive cycles of 0.2 nm steps within 1 and 5 ms pauses). The stiffness of the tip was 20 pN nm^{-1}, corresponding to a loading rate of approximately 700 pN s^{-1}. The distribution of the unbinding forces was bimodal with the peaks at 14.8 ± 4.0 pN and 24.7 ± 1.4 pN, which corresponded to the single-headed and the double-headed binding, respectively. These values are higher than those reported by Nishizaka *et al.* (1995, 2000), which is attributable to the higher loading rates used in this study.

A more recent study probed the force-dependent kinetics of actomyosin bond in the rigour (nucleotide-free) state or the ADP-bound state in a wide range of loading

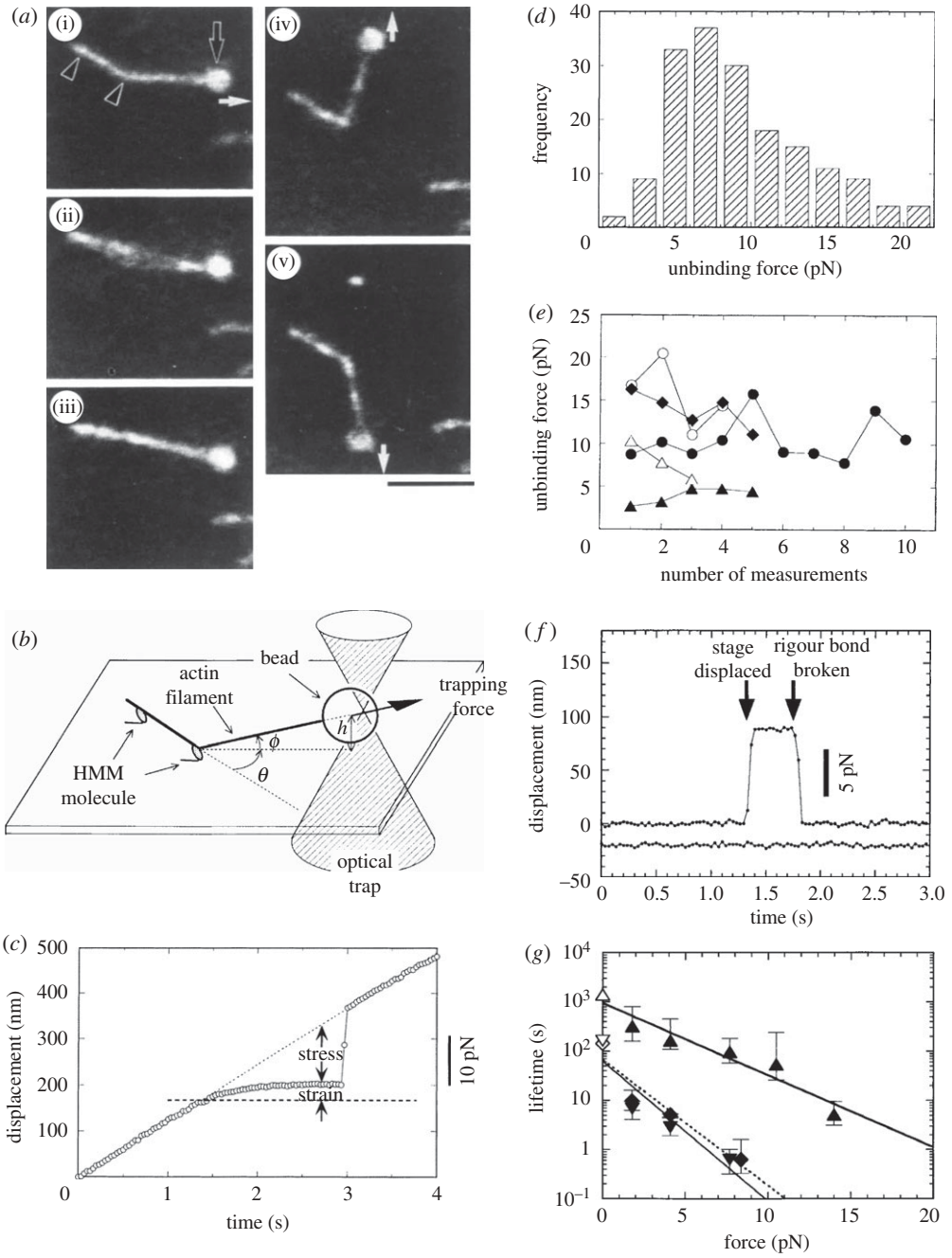

Figure 1. Single-molecule response of actomyosin bonds to load. (*a*) A series of fluorescence micrographs showing the measurement of the unbinding force of a rigour bond(s) between an actin filament and a single HMM molecule. The bead (indicated by the black arrow in (i)) was trapped by a single laser beam and moved at a constant rate in the direction indicated by the white arrow, such that the actin filament became taut. The actin filament was attached to the surface by two separate HMM molecules identified as two nodal points (black arrowheads in (i)). As the laser spot was further moved, the load on the nearest HMM molecule increased and subsequently one of the two molecules unbound (ii), such that the filament became nearly straight (iii). The actin filament could be reattached to the same position while the second molecule was still attached, and the external loads could be imposed in any direction, as indicated by the white arrows (iv,v). Scale bar, 5 μm. (*b*) Schematic illustration of (*a*): θ is the angle of the applied force, h (less than 1 μm) is the distance between the bead and a glass surface ($\theta \leq 10^{\circ}$). (*c*) Time course of the movement of the trap centre (dotted line, 120 nm s^{-1}, corresponding to an approximately 12 pN s^{-1} loading rate) and the trapped bead (circles) to which an actin filament was attached. The unbinding force between an actin filament and an HMM molecule was estimated from the abrupt displacement at 2.9 s, when the rigour bound was ruptured. (*d*) Histogram of the unbinding forces between a single actin filament and a single HMM molecule. (*e*) Effect of the number of measurements. Different symbols represent different HMM molecules. (*f*) An example of the time course of the displacement of the bead. The upper and the lower plots show, respectively, the displacement of the bead along and perpendicular to the actin filament. The stage was displaced stepwise at 1.3 s to impose a constant external load, and the bond ruptured after 0.43 s in this example. (*g*) Relation between the imposed load and the lifetime of HMM and S1 rigour bonds. Triangles and inverted triangles show the slow and the fast components of HMM, respectively. Diamonds show the lifetime of S1. The thick and thin solid lines show the approximation of slow and fast components of HMM, respectively. The dashed line shows the approximation for S1. (Adapted from Nishizaka *et al.* 1995, 2000).

rates (Guo & Guilford 2006). The authors observed that over the physiological range of rapidly applied loads, the actomyosin bond behaved as a 'catch' bond, which is characterized by the longer lifetimes with increasing load up to approximately 6 pN, which is near the value of force generated by an individual myosin molecule during isometric contraction (figure 2). Furthermore, at high loading rates, the actomyosin–ADP bond surprisingly possessed longer lifetimes than the rigour bond. The authors propose that actomyosin bonds and possibly all 'catch' bonds between the load-bearing molecules are tuned to their physiological environment. However, in this study, load was applied perpendicularly to the actin filament's axis (figure 2), which leaves open the question whether these intriguing findings are applicable to the actual physiological processes, but nevertheless they may turn out to be important for the currently unknown applications of the molecular motors.

2.2. Probing the mechanism of the processive motors

During one cycle of ATP hydrolysis, molecular motors form different conformations with different affinities for their substrate filaments and alternate binding and unbinding. These properties were exploited in a series of experiments probing the mechanism of the processive motors, kinesin and myosins V and VI.

The initial work of this series (Kawaguchi & Ishiwata 2001) focused on testing the major prediction of the 'hand-over-hand' model (figure 3*a*) of the kinesin motility by directly determining the binding mode of single native kinesin molecules at three different solvent conditions: in the absence of nucleotides (with some number of ADP-bound heads), in the presence of the non-hydrolysable ATP analogue, adenosine 5′-(β,γ-imido) triphosphate (AMP–PNP) and in the coexistence of AMP–PNP and ADP. The binding mode was determined by slowly displacing a kinesin-bound bead, trapped with optical tweezers, along a polarity-labelled microtubule immobilized on the glass surface. The rate of the bead's movement was kept constant at 120 nm s^{-1}, which corresponded to the loading rate of 10.4 pN s^{-1}. For the determination of the binding mode, two parameters have been analysed: (i) the unbinding force, determined from the displacement of a bead from the trap centre at the rupture point of the kinesin–microtubule complex; and (ii) the elastic modulus of the kinesin–microtubule complex, determined from the slope of the force–extension relation, which was found to be almost linear. The distributions of both the unbinding forces and the elastic modulus at all three solvent conditions unequivocally revealed that kinesin binds with a single head both in the absence of nucleotides and in the coexistence of AMP–PNP and ADP, whereas the binding in the presence of AMP–PNP is predominantly double-headed, though rare single-headed unbinding events were also detected (figure 3*b–g*). At all three nucleotide states, the unbinding forces for the minus end-directed loading were approximately 45 per cent larger than under the plus-end-directed loading, which suggested that in the

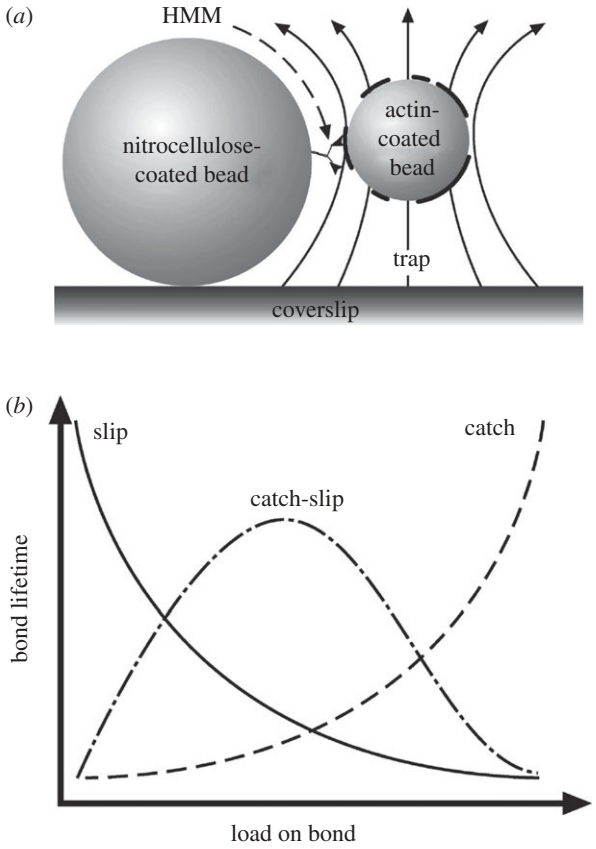

Figure 2. Force spectroscopy of actomyosin bonds under perpendicularly applied load. (*a*) Schematic showing the arrangement for actomyosin force spectroscopy using the laser trap. (*b*) Illustration of the expected responses of catch, slip and catch–slip bonds to imposed loads when measured in terms of bond lifetime. (Adapted from Guo & Guilford 2006.)

'bridge' structure of kinesin, with both heads bound to a microtubule, the trailing head binds a microtubule less stably, tending to detach. This difference in the mechanical stability of the attachment of the leading and the trailing heads to a microtubule was suggested to be essential for the mechanism of the unidirectional motility of kinesins.

An interesting observation made in that study was that the proportion of the single-headed binding in the AMP–PNP state gradually decreased with an increase in loading rate and eventually disappeared at the highest examined loading rate (18 pN s^{-1}), suggesting that in the absence of the external load, the double-headed binding is predominant and there exists an equilibrium between the single- and the double-headed binding. A careful investigation of how the binding mode of kinesin depends on the loading rate was performed in the later study (Kawaguchi *et al.* 2003). In this work, the binding in the absence of nucleotides or in the presence of AMP–PNP was tested in a wide range of loading rates (from approx. 3.5 pN s^{-1} up to greater than 50 pN s^{-1}; figure 4*a*). Load was exerted on individual kinesin–microtubule complexes either by displacing the trap centre, as in previous studies, or to exert highest tested loading rates of greater than 50 pN s^{-1}, by moving a microscope

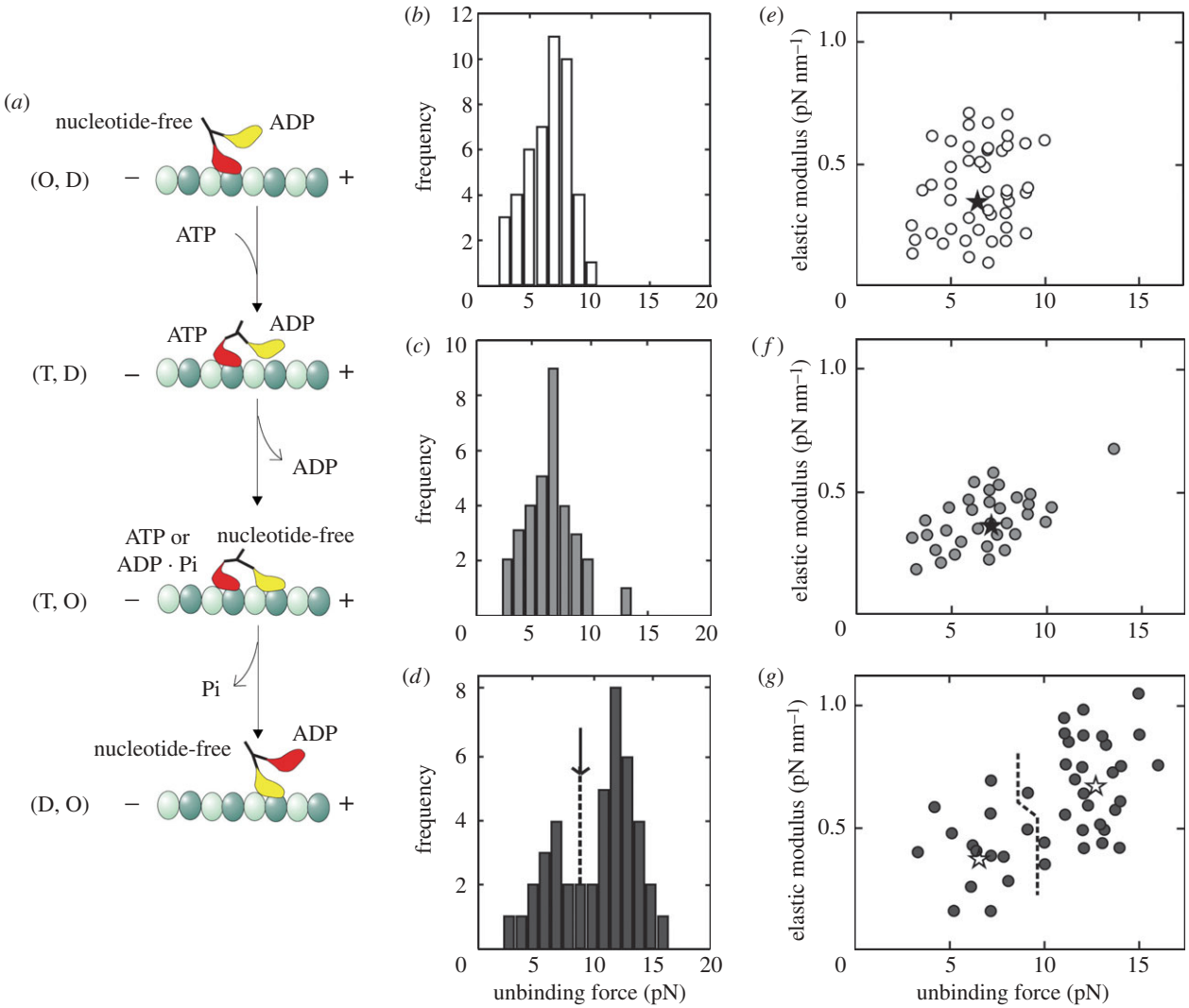

Figure 3. Experiments probing the major prediction of the 'hand-over-hand' model of kinesin motility. (*a*) A simplified version of the 'hand-over-hand' model on the mechanism of kinesin motility. O, nucleotide free; D, T and Pi, ADP, ATP and inorganic phosphate, respectively. Distribution of unbinding force (*b*–*d*) and relation between elastic modulus and unbinding force (*e*–*g*) at different nucleotide-bound states. The external load was applied toward the plus end. (*b*,*e*) Nucleotide-free ($n = 46$); (*c*,*f*) AMP–PNP + ADP ($n = 33$); (*d*,*g*) + AMP–PNP ($n = 43$). Unbinding force (pN) ± s.d.: 6.7 ± 1.8 (*b*), 7.2 ± 2.0 (*c*), 6.6 ± 1.7 ($n = 14$), 12.8 ± 1.6 ($n = 29$) (*d*). Elastic modulus (pN nm^{-1}) ± s.d.: 0.35 ± 0.14 (*e*), 0.37 ± 0.16 (*f*) and 0.39 ± 0.17 ($n = 14$), 0.67 ± 0.21 ($n = 29$) (*g*). Loading rate (pN s^{-1}): 3.5 (*b*,*e*), 6.0 (*c*,*f*) and 4.3 (*d*,*g*). A single Gaussian distribution could simulate unbinding force distribution in (*b*,*c*). In contrast, the unbinding force distribution in (*d*) was simulated by the sum of two Gaussian distributions, with S- and L-components defined as the smaller and larger unbinding force, respectively. The boundary between the S- and L-components was determined by the junction of two Gaussian distributions (shown by an arrow (*d*)); the boundary in (*g*) was determined according to that in (*d*). The average values for S- and L-components are shown by asterisks in (*e*)–(*g*). (Adapted from Kawaguchi & Ishiwata 2001.)

stage with a sample fixed on it. Loads were applied towards both the plus end and the minus end of the microtubule. The fast exertion of load allowed taking snapshots of the binding mode at the binding equilibrium in the absence of the external load, that is, before any transitions between the single- and the double-headed binding states occur. The measurements at high loading rates revealed that in the absence of nucleotides, the binding distribution is bimodal, that is, both the single- and the double-headed binding coexist (figure 4*b*); at the same time, in the presence of AMP–PNP at the highest examined loading rate (18 pN s^{-1}), only the double-headed binding was detected, irrespective of the loading direction. However, a decrease in the loading rate significantly changed the shape of the distributions at both solvent conditions; specifically, in the absence of nucleotides, the peak corresponding to the double-headed binding disappeared. On the contrary, in the presence of AMP–PNP, with a decrease in the loading rates, the single-headed binding was also detected in addition to the double-headed binding, and the peak for the single-headed binding became more prominent as the loading rate was decreasing.

These observations suggested that there exists an equilibrium between the single-headed and the double-headed binding, and the experimentally obtained unbinding force distributions were used to

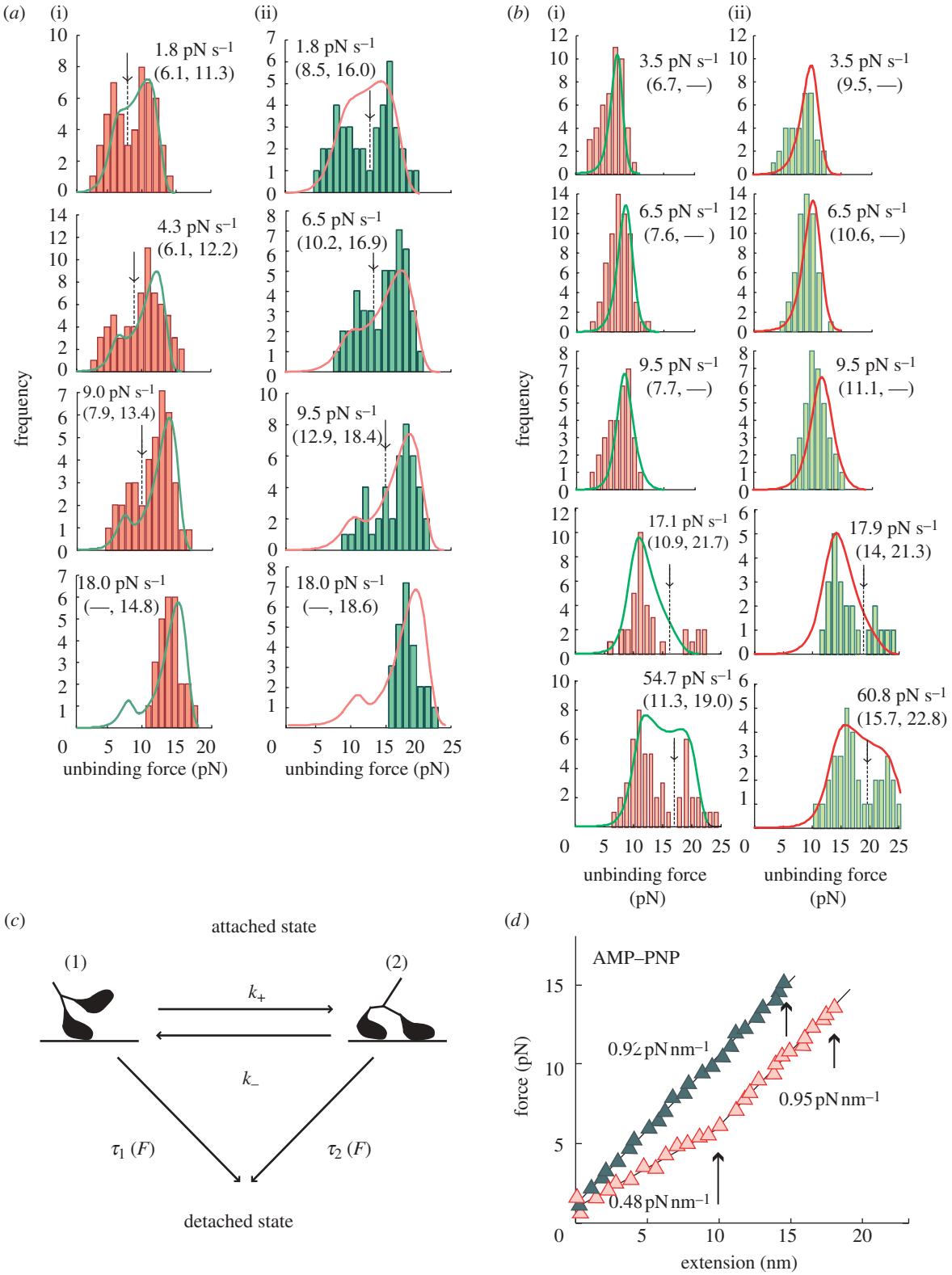

Figure 4. Binding mode of kinesin depends on loading rate. (*a*) Loading rate dependence of the unbinding force distribution in the AMP–PNP state. Unbinding force was measured by loading towards either the plus end (*a*(i)) or the minus end (*a*(ii)). (*b*) Loading rate dependence of the unbinding force distribution in the nucleotide-free state. Unbinding force was measured by loading towards either the plus end (*b*(i)) or the minus end (*b*(ii)). (*c*) Scheme to explain the dependence of the average unbinding force and the unbinding force distributions on loading rate and loading direction. A model where equilibrium is assumed to exist between the single-headed (1) and the double-headed (2) binding with the rate constants, k_+ and k_-, between two binding states. (*d*) Relation between the elastic modulus and unbinding force of kinesin molecules measured by the plus-end loading in the AMP–PNP state. Examples showing the force-extension relation obtained from the time course of bead displacement for the initial unbinding (dark green) and the subsequent unbinding (pink) that were observed during the movement of the kinesin-bound bead by manipulating with the laser trap along a microtubule at a constant rate. Short arrows show the moment at which the detachment of kinesin occurred. Long arrow shows the moment at which the transition to a steeper slope occurred. (Adapted from Kawaguchi *et al.* 2003.)

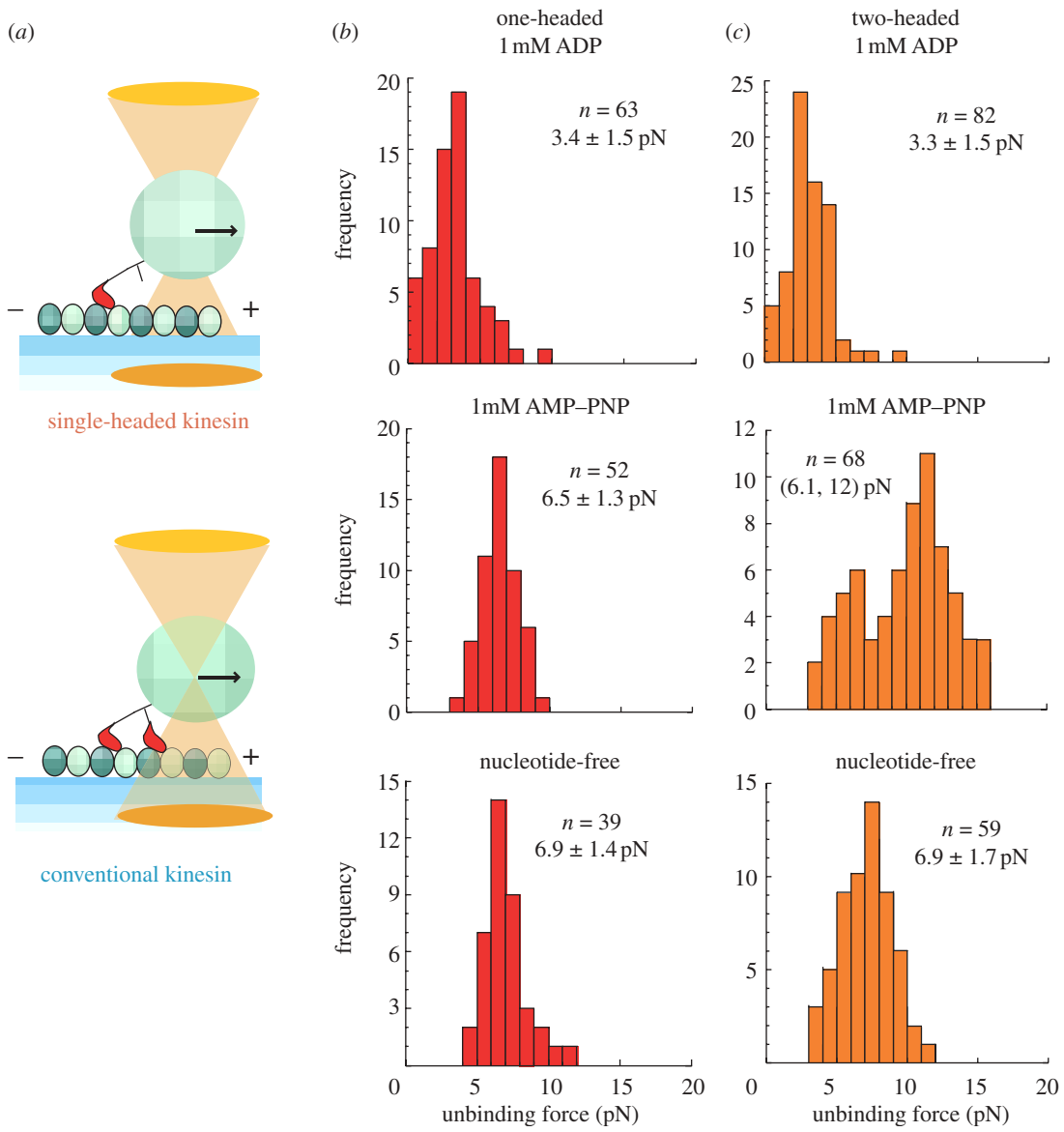

Figure 5. Unbinding forces of the single- and the double-headed kinesins. (*a*) Schematic illustration showing the method of application of external load to one-headed or two-headed kinesin-coated bead by using optical tweezers. The relative size of the bead compared with kinesin is reduced to about one-tenth of the actual scale. In this illustration, the load is applied towards the plus-end of a microtubule. Unbinding-force distribution for (*b*) one-headed kinesin and (*c*) conventional two-headed kinesin at several nucleotide states towards the plus-end of the microtubule. (Adapted from Uemura *et al.* 2002.)

successfully test a model, which postulated the existence of such equilibrium both in the nucleotide-free and the AMP–PNP-bound states (figure 4*c*). The lifetime of the bond, τ, in this model is load-dependent, such that, as in the case of the actin–myosin interaction, $\tau(F) = \tau(0)\exp(-Fd/k_{\mathrm{B}}\mathrm{T})$, where $\tau(0)$ is the bond lifetime in the absence of external load, F is the applied load and d is the characteristic distance of the kinesin–microtubule interaction. The model predicted that the forward and the backward rates of the transition from the single- to the double-headed binding were 70 and 7 s^{-1}, respectively, for the nucleotide-free state, and 2 and 0.2 s^{-1} for the AMP–PNP state, under the assumption that the ratio of forward to backward transition rates is 10. The experimentally obtained transition rate in the presence of AMP–PNP, determined from an abrupt increase in the elastic modulus, was estimated to be approx. 1 s^{-1}, showing good agreement with the model (figure 4*d*). Besides, the same analysis demonstrated that initially kinesin binds to a microtubule with a single head, followed by a transition to the double-headed binding.

These experiments were further developed by using the recombinant one-headed kinesin construct (Uemura *et al.* 2002). These measurements were performed separately with both the one-headed construct and the native two-headed kinesin (figure 5*a*), at three different solvent conditions: in the presence of saturating concentrations (1 mM) of ADP or AMP–PNP, or in the absence of nucleotides (figure 5*b*,*c*). The only major difference in the unbinding force distributions observed between the one-headed and the two-headed kinesin molecules, was the bimodality of the distribution in the AMP–PNP state of the two-headed kinesin, which confirmed the conclusion that the two peaks correspond to the single- and the

double-headed binding (Kawaguchi & Ishiwata 2001). This study also confirmed that the binding in the ADP state is significantly weaker than in the nucleotide-free or in the AMP–PNP-bound state. The model analysis based on the experimental results yielded the characteristic distance, d, being 4.0 and 3.0 nm, respectively, for the forward and the backward loading; importantly, these values did not depend on the nucleotide state, implying the existence of an intrinsic asymmetry in the mechanical stability of the attachment of the leading and the trailing heads of kinesin to a microtubule. For example, under a 4 pN load, the trailing head would detach approximately threefold more easily than the leading head, which was predicted to be an important factor assisting the efficient processive motility of kinesin and, possibly, other dimeric motors.

Another feature of the mechanism, enabling the dimeric processive motors to move unidirectionally on their tracks, was suggested to be the asymmetry in the enzymatic properties, such as binding of ATP and the products of its hydrolysis, between the two heads (Hackney 1994). This prediction was tested experimentally (Uemura & Ishiwata 2003) by applying load to individual kinesin–microtubule complexes in the range of ADP concentrations (0–1 mM), towards either the plus-end or the minus-end of a microtubule. In this work, two important features of the kinesin–microtubule interaction, discovered in the earlier studies, have been exploited: first, the binding in the ADP state is weaker than in the nucleotide-free state (Uemura *et al.* 2002), and second, the loading rate was kept sufficiently low (5.5 ± 0.14 pN s^{-1}), that is, slower than the rates of ADP binding and dissociation, as well as the rates of the transition between the single- and the double-headed binding (Uemura *et al.* 2002; Kawaguchi *et al.* 2003); these conditions ensured that the distributions of the unbinding force exclusively contained the weak, single-headed binding state (ADP-bound) and the strong and also single-headed nucleotide-free binding state. The positions of these two peaks remained constant at all tested ADP concentrations (0, 1, 10, 100 and 1000 μM); however, the relative population of the two states varied with the ADP concentration and, most importantly, depended also on the loading direction, such that the strong-binding peak, corresponding to the unbinding in the nucleotide-free state, appeared at lower ADP concentration under the minus end-directed load. The proportion of the ADP-bound state for the two loading directions, plotted against the ADP concentration, could be fit with a hyperbola, which yielded the asymmetric apparent ADP affinities for the plus-end and the minus-end loading (12.7 ± 2.4 and 86.0 ± 17.1 μM, respectively). These values indicate that ADP dissociates more readily from the leading head than from the trailing head, which agrees with the 'hand-over-hand' model of the kinesin motility (figure 6).

Another series of studies probed the motility mechanism of the processive myosins V and VI. Myosin V is a robust intracellular transporter, which moves cargos towards the cell periphery, whereas myosin VI

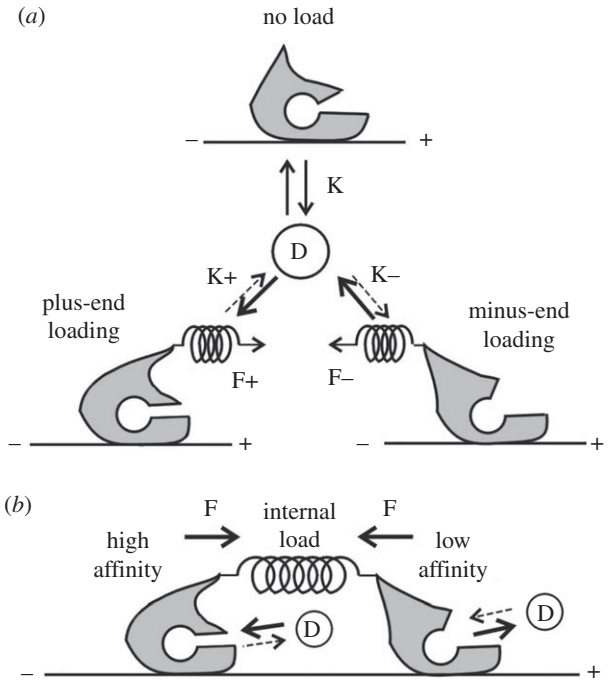

Figure 6. Schematic illustrations showing equilibrium of ADP (D) binding to a kinesin–microtubule complex. (*a*) The effect of imposing load towards the plus end (F+) or the minus end (F−) of a microtubule on the binding equilibrium. The dissociation constants of ADP in a kinesin–microtubule complex in the absence of load (K), under plus-end loading, K+ and under minus-end loading, K−, are shown. (*b*) A possible role of an internal load within a two-headed kinesin molecule on the binding equilibrium. In (*b*), such a situation is illustrated that the internal load, which may be produced by extension of the link between the two heads upon binding to a microtubule, increases the binding affinity of ADP for the trailing head (left side) and decreases that for the leading head (right side). The internal load between the two heads is assumed to be equivalent to the plus-end loading for the trailing head and the minus-end loading for the leading head. (Adapted from Uemura & Ishiwata 2003.)

in cells seems to play a dual role of either an anchor or an oppositely directed vesicle transporter. First, the binding mode of native myosin V molecules in the absence of nucleotides or in the presence of saturating ADP (1 mM) was examined (Mikhailenko *et al.* 2008; figure 7*a–c*). In these experiments load was applied towards the barbed end of an actin filament, that is, in the direction of myosin's stepping, by displacing the microscope stage. As a control, a recombinant myosin V-S1 (1IQ) construct was used. Both in the nucleotide-free and in the ADP-bound states, the distributions for the native myosin V were bimodal, showing the occurrence of both the single-headed and the double-headed binding (figure 7*d–g*). Interestingly, the force required for rupturing the double-headed binding was significantly larger than twice the value of the rupture force of the single-headed binding (13.6 and 4.3 pN, respectively). The necessity to apply the additional 5 pN may indicate that the presence of the second head reduces the effective load on the actin-binding interface, stabilizing the double-headed bound conformation.

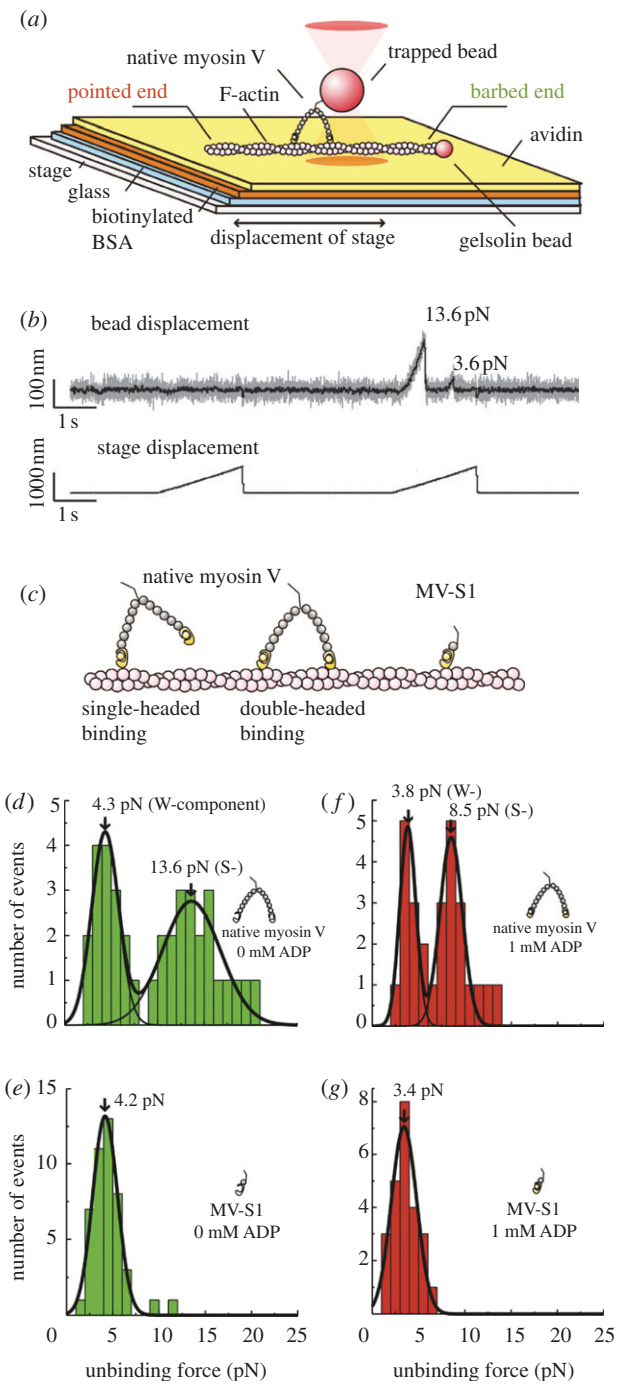

Figure 7. Measurements probing the binding mode of myosin V. (*a*) Schematic illustration of the experimental system. A polystyrene bead (diameter 1 μm), to which a single myosin molecule (native myosin V or single-headed MV-S1) is attached, is held with optical tweezers and brought close to a 10 per cent-biotinylated actin filament, immobilized on a glass surface via the biotin–avidin interaction. The polarity of the actin filament was determined using a gelsolin-coated bead (diameter 0.2 μm), which specifically attaches to its barbed end. (*b*) A typical trace of bead displacement for native myosin V in the nucleotide-free state. Both the double- and the single-headed interactions were detected during the same pulling event. (*c*) Schematic representation of the binding modes of native myosin V and of the MV-S1 construct. Unbinding force distributions for native myosin V in the nucleotide-free (*d*) and the ADP-bound state (*f*) and for single-headed MV-S1 in the nucleotide-free (*e*) and the ADP-bound state (*f*). (Adapted from Mikhailenko *et al.* 2008.)

Another study examined the loading direction-dependence of the ADP affinity in myosins V and VI (Oguchi *et al.* 2008). The recombinant single-headed constructs, myosin V–6IQ and myosin VI–1IQ, were used, and the experimental set-up was the same as in the previous study (Mikhailenko *et al.* 2008). Similar to an earlier work on kinesin (Uemura & Ishiwata 2003), the unbinding forces were measured at several ADP concentrations, under load applied towards either the barbed or the pointed end of actin. The rupture force distributions were globally fitted with a sum of two Gaussians, corresponding to the unbinding in the weaker (ADP-bound) or the stronger (nucleotide-free) binding states, and the proportion of the ADP-bound state was determined as the area of the corresponding peak divided by the total area of each distribution. The apparent ADP dissociation constants (K_d), determined by the hyperbolic fits of the proportion of the ADP state plotted against the ADP concentration, indicated that the directional load asymmetrically affected the ADP binding. The values of K_d were 1.2 ± 0.2 and 23 ± 3.7 μM (for myosin V) or 6.8 ± 1.4 and 17.2 ± 3.6 μM (for myosin VI) under the backward and the forward loads, respectively, suggesting that these two motors, despite being oppositely directed, are similarly controlled by the asymmetric binding of ADP between the two heads, such that ADP is more tightly bound to the leading head.

The next important question, which had to be addressed, was whether this asymmetry originates from the inhibited dissociation from the leading head, or from the accelerated dissociation from the trailing head, or both these factors are involved. As $K_d = k^-_{ADP}/k^+_{ADP}$, where k^-_{ADP} and k^+_{ADP} are the rates of the ADP dissociation and binding, respectively, both of which may be load-dependent, the comparison of the K_d values with those obtained in the solution studies under no load, did not provide sufficient information on which of the heads was affected by load. Therefore, the load-dependence of the rates of ADP dissociation and binding was revealed by the model analysis, based on the assumption that both the dissociation and binding of ADP, as well as the lifetime of the actomyosin bond in both the nucleotide-free and the ADP-bound state, follow the Bell equation. Such analysis revealed that in myosin V, the ADP dissociation from the leading head is strongly (greater than 20-fold) inhibited by an approximately 2 pN-load, whereas the ADP dissociation from the trailing head is accelerated only marginally (less than twofold), providing strong support for the model in which the efficient processive movement of myosin V is achieved by trapping the leading head in the ADP state, which strongly binds with actin. In myosin VI, the asymmetry in the ADP dissociation rates between the heads was smaller, which hints at the possibility that the efficiency of its processive movement might be helped by another factor, such as the asymmetric rates of ATP binding. However, another possible explanation is that the lever arm of the construct used in this study was not sufficiently long, being cut immediately after the IQ motif. The later study on myosin V (Oguchi *et al.* 2010) revealed that the lever must be long to create a

large asymmetry in the ADP dissociation rates between the two heads, and the short 1IQ lever is unable to strongly inhibit ADP dissociation from the leading head, similar to the short-lever myosin VI construct. The long single α-helix (SAH), which follows the IQ motif in myosin VI, was shown to perform like a long lever arm (Spink *et al.* 2008), which raises the possibility that the unbinding force measurements performed with a longer construct containing the SAH would reveal the larger asymmetry between the two heads in myosin VI owing to the stronger inhibition of the ADP release from the leading head.

In this work, both forward and backward loads were found to be accelerating the ADP binding to myosin VI, but inhibit it to myosin V. This is consistent with myosin VI playing an anchoring role under external loads in cells (Altman *et al.* 2004).

A recent study (Gebhardt *et al.* 2010) reported that the stabilities of rigour bonds between an actin filament and single-headed myosin V (6IQ or 4IQ) constructs are strongly asymmetrical, being, in the case of the 6IQ construct, 1.7 and 4.2 pN, respectively, under the backward and the forward loads. This observation was suggested to explain the observed different response of the dimeric myosin V to high mechanical loads (Gebhardt *et al.* 2006), which were reported to induce processive steps even in the absence of ATP when applied in the backward direction, whereas the analogous forward steps could not be induced. These strongly asymmetrical stabilities were not detected in the previous study, which reported the unbinding forces of 5.1 and 4.6 pN under the backward and the forward loading, respectively (Oguchi *et al.* 2008). This discrepancy was suggested to originate from the differences in the experimental protocols, such as the manner of the attachment of the myosin molecules to the beads or an actin filament to the glass surface.

The latest study (Oguchi *et al.* 2010) thoroughly examined the properties of an actomyosin V bond in the nucleotide-free or the ADP-bound state under the diagonally applied loads (figure 8). Myosin V is a highly efficient intracellular transporter, able to swiftly adjust to variable 'road' conditions when moving across the dense cellular environment. However, little was known about how load-induced regulation of the processive stepping occurs *in vivo*, where myosin V likely experiences significant intramolecular and external off-axis loads, such as during track-switching at the intersections, or when following the left-handed helix around an actin filament (Ali *et al.* 2002), or dragging cargo through a dense cellular network. This study revealed that myosin V remains highly processive under loads applied in various directions, owing to a strongly inhibited ADP dissociation from the leading head, and that the native 6IQ lever is indispensable for the efficient loading direction-independent inhibition of the ADP dissociation from the leading head. These measurements also provided a possible explanation for the discrepancy in the reported stabilities of actomyosin V–6IQ bonds under the directional loads, mentioned in the previous paragraph, by observing that these stabilities strongly depend on the loading angle (figure 8*c*). It is conceivable that a complex geometry of the myosin's attachment to the bead (Gebhardt *et al.* 2010), which used a C-terminal YFP bound to the bead's surface via a GFP antibody, might have produced an additional asymmetry in the direction-dependent stabilities, as well as a certain angle for the myosin–actin bond. Such undesirable effects are less plausible if a small *c-myc* tag is used, which is supported by a good correlation between the effects of the diagonal (-20° and $+20^\circ$) loads on the load-dependent properties of a single-headed myosin V–6IQ molecule, attached to the beads via *c-myc* tags, and on the manner of the processive stepping of native myosin V molecules, non-specifically bound to beads, in the optical trap (Oguchi *et al.* 2010).

2.3. Probing the motor–track interaction on the modified 'tracks'

The measurements of the unbinding force were used for the identification of the strongly binding sites for kinesin on a microtubule using the mutational analysis of tubulin (Uchimura *et al.* 2006). Using the budding yeast expression system, the authors prepared the mutated β-tubulin constructs, replacing the negatively charged residues in the α-helix 12, which was suggested to be critical for the kinesin–microtubule interaction, with alanines. The rupture force measurements revealed that in the E410A, D417A and E421A mutants, but not in the E412A mutant, the kinesin–microtubule binding became less stable in the AMP–PNP-bound state under load applied towards the microtubule minus end, correlating with the observed reduction in the affinity of the microtubules for kinesin, implying that the former three residues are critical for the kinesin–microtubule interaction in the strong binding state.

In another valuable work, the rupture forces were measured between the ribosome, a complex catalytic machine, and its track, the messenger RNA, to examine the contribution of the Sine–Dalgarno (SD) sequence on the mRNA and to gain insights to the mechanism of the mRNA–ribosome interaction (Uemura *et al.* 2007). These measurements revealed that the removal of the SD sequence drastically decreased the rupture forces in complexes containing an aminoacyl tRNA, Phe-tRNA^{Phe}, at the aminoacyl-tRNA site (A-site), indicating that prior to the peptide bond formation, the SD interactions significantly contribute to the stability of the ribosomal complex on the mRNA. In contrast, when the A-site contained a peptidyl tRNA analogue, *N*-acetyl-Phe-tRNA^{Phe}, which mimicked the post-peptidyl transfer state, the rupture forces were weaker when compared to the complex with Phe-tRNA^{Phe}, and did not depend on the presence or absence of the SD sequence, suggesting that the formation of the first peptide bond destabilizes the SD interaction, consequently weakening the binding between the ribosome and an mRNA.

3. CONCLUSIONS

The studies reviewed here demonstrate that the measurements of the unbinding force can reveal

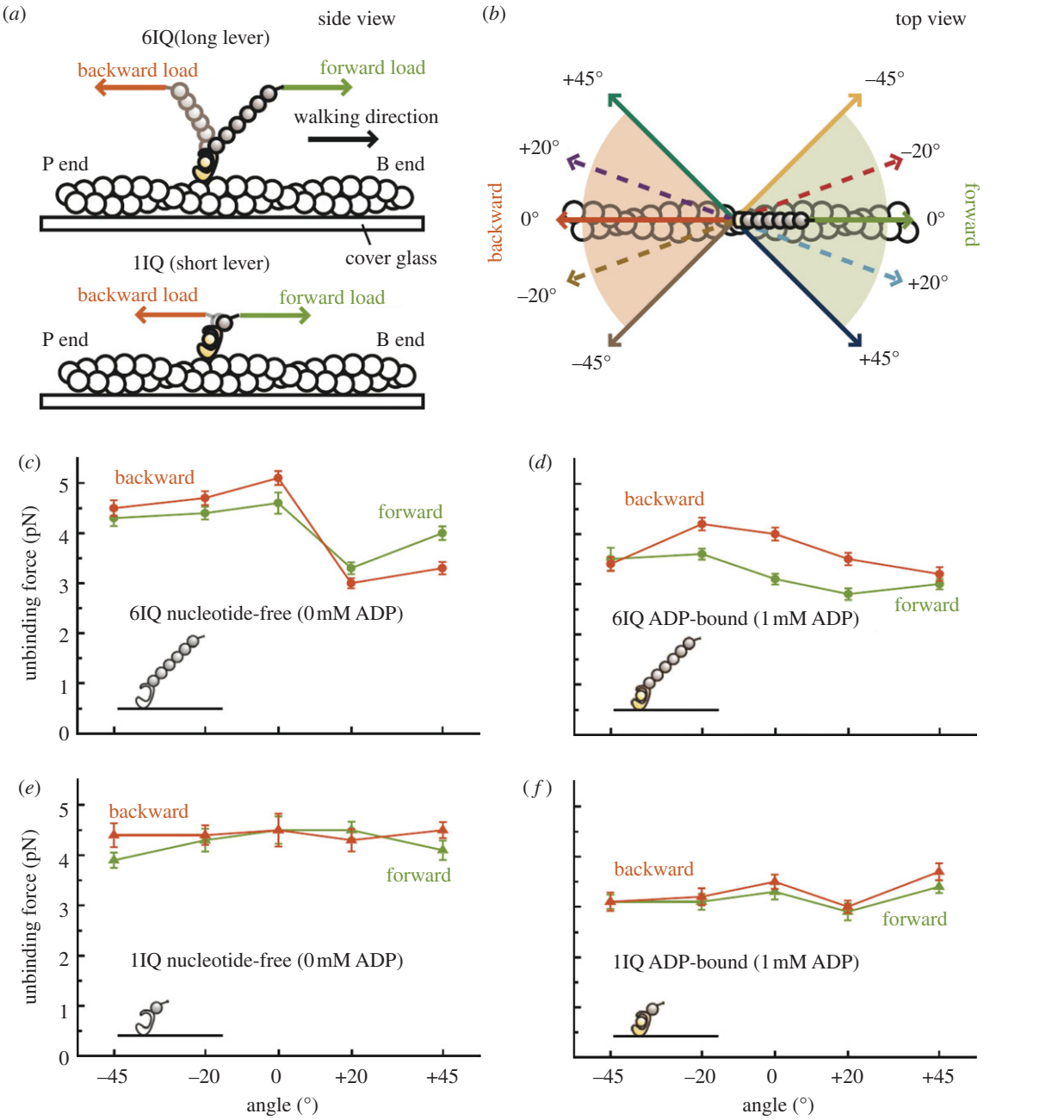

Figure 8. Effect of the off-axis loads on the actomyosin V–6IQ interaction. (*a*) Constructs used in this study (side view). (*b*) The tested loading angles (top view). Dependence of the unbinding force on loading angle. (*c*,*d*) The 6IQ construct in the nucleotide-free state (*c*) and the ADP-bound state (*d*). (*e*,*f*) The 1IQ construct in the nucleotide-free state (*e*) and the ADP-bound state (*f*). (Adapted from Oguchi *et al.* 2010.)

important insights into the various aspects of the motor–track interaction and, certainly, of the processes in other biological systems as well. The results obtained using this technique stress the importance of the experimental geometry in the single-molecule measurements, and future studies should attempt to provide as much control of the direction of force application as possible, which will undoubtedly lead to the surprising and unexpected results, helping the researchers to deepen our understanding of the processes taking place in various biological systems. It has already been shown that loads imposed on the processively stepping myosin V (Gebhardt *et al.* 2006) and kinesin (Carter & Cross 2005) molecules significantly change the manner of their processive stepping, even being able to reverse its direction. The loads applied not along the direction of the motors' movement, but off-axis and even perpendicularly, may reveal unique features of the motor–track interaction and provide a valuable means of controlling the motors' performance, which in near future may find application in novel fields of nanotechnology.

This work was supported by the Grants-in-Aid for Specially Promoted Research, Scientific Research (A) and the 'Academic Frontier' Project from the Ministry of Education, Culture, Sports, Science and Technology of Japan to S.I. Y.O. is a research fellow of the Japan Society for the Promotion of Science.

REFERENCES

Ali, M. Y., Uemura, S., Adachi, K., Itoh, H., Kinosita Jr, K. & Ishiwata, S. 2002 Myosin V is a left-handed spiral motor on the right-handed actin helix. *Nat. Struct. Biol.* **9**, 464–467. (doi:10.1038/nsb803)

Altman, D., Sweeney, H. L. & Spudich, J. 2004 The mechanism of myosin VI translocation and its load-induced anchoring. *Cell* **116**, 737–749. (doi:10.1016/S0092-8674(04)00211-9)

Ashkin, A., Dziedzic, J. M., Bjorkholm, J. E. & Chu, S. 1986 Observation of a single-beam gradient force optical trap for dielectric particles. *Opt. Lett.* **11**, 288–290. (doi:10.1364/OL.11.000288)

Bell, G. I. 1978 Models for the specific adhesion of cells to cells. *Science* **200**, 618–627. (doi:10.1126/science.347575)

Carter, N. J. & Cross, R. A. 2005 Mechanics of the kinesin step. *Nature* **435**, 307–312. (doi:10.1038/nature03528)

Deniz, A. A., Mukhopadhyay, S. & Lemke, E. A. 2008 Single-molecule biophysics: at the interface of biology, physics and chemistry. *J. R. Soc. Interface* **5**, 15–45. (doi:10.1098/rsif.2007.1021)

Erickson, H. P. 1994 Reversible unfolding of fibronectin type III and immunoglobulin domains provides the structural basis for stretch and elasticity of titin and fibronectin. *Proc. Natl Acad. Sci. USA* **91**, 10 114–10 118. (doi:10.1073/pnas.91.21.10114)

Finer, J. T., Simmons, R. M. & Spudich, J. A. 1994 Single myosin molecule mechanics: piconewton forces and nanometre steps. *Nature* **368**, 113–119. (doi:10.1038/368113a0)

Florin, E. L., Moy, V. T. & Gaub, H. E. 1994 Adhesion forces between individual ligand-receptor pairs. *Science* **264**, 415–417. (doi:10.1126/science.8153628)

Gebhardt, J. C., Clemen, A. E., Jaud, J. & Rief, M. 2006 Myosin-V is a mechanical ratchet. *Proc. Natl Acad. Sci. USA* **103**, 8680–8685. (doi:10.1073/pnas.0510191103)

Gebhardt, J. C., Okten, Z. & Rief, M. 2010 The lever arm effects a mechanical asymmetry of the myosin-V-actin bond. *Biophys. J.* **98**, 277–281. (doi:10.1016/j.bpj.2009.10.017)

Guo, B. & Guilford, W. H. 2006 Mechanics of actomyosin bonds in different nucleotide states are tuned to muscle contraction. *Proc. Natl Acad. Sci. USA* **103**, 9844–9849. (doi:10.1073/pnas.0601255103)

Hackney, D. D. 1994 Evidence for alternating head catalysis by kinesin during microtubule-stimulated ATP hydrolysis. *Proc. Natl Acad. Sci. USA* **91**, 6865–6869. (doi:10.1073/pnas.91.15.6865)

Ishijima, A., Harada, Y., Kojima, H., Funatsu, T., Higuchi, H. & Yanagida, T. 1994 Single-molecule analysis of the actomyosin motor using nano-manipulation. *Biochem. Biophys. Res. Commun.* **199**, 1057–1063. (doi:10.1006/bbrc.1994.1336)

Kawaguchi, K. & Ishiwata, S. 2001 Nucleotide-dependent single- to double-headed binding of kinesin. *Science* **291**, 667–669. (doi:10.1126/science.291.5504.667)

Kawaguchi, K., Uemura, S. & Ishiwata, S. 2003 Equilibrium and transition between single- and double-headed binding of kinesin as revealed by single-molecule mechanics. *Biophys. J.* **84**, 1103–1113. (doi:10.1016/S0006-3495(03)74926-1)

Kishino, A. & Yanagida, T. 1988 Force measurements by micromanipulation of a single actin filament by glass needles. *Nature* **334**, 74–76. (doi:10.1038/334074a0)

Mikhailenko, S. V., Oguchi, Y., Ohki, T., Shimozawa, T., Olivares, A. O., De la Cruz, E. M. & Ishiwata, S. 2008 How the load and the nucleotide state affect the actin filament binding mode of the molecular motor myosin V. *J. Kor. Phys. Soc.* **53**, 1726–1730. (doi:10.3938/jkps.53.1726)

Miyata, H., Yoshikawa, H., Hakozaki, H., Suzuki, N., Furuno, T., Ikegami, A., Kinosita Jr, K., Nishizaka, T. & Ishiwata, S. 1995 Mechanical measurements of single actomyosin motor force. *Biophys. J.* **68**, 286S–289S.

Molloy, J. E., Burns, J. E., Kendrick-Jones, J. R., Tregear, T. & White, D. C. S. 1995 Movement and force produced by a single myosin head. *Nature* **378**, 209–212. (doi:10.1038/378209a0)

Nakajima, H., Kunioka, Y., Nakano, K., Shimizu, K., Seto, M. & Ando, T. 1997 Scanning force microscopy of the interaction events between a single molecule of heavy meromyosin and actin. *Biochem. Biophys. Res. Commun.* **234**, 178–182. (doi:10.1006/bbrc.1997.6612)

Nishizaka, T., Miyata, H., Yoshikawa, H., Ishiwata, S. & Kinosita Jr, K. 1995 Unbinding force of a single motor molecule of muscle measured using optical tweezers. *Nature* **377**, 251–254. (doi:10.1038/377251a0)

Nishizaka, T., Seo, R., Tadakuma, H., Kinosita Jr, K. & Ishiwata, S. 2000 Characterization of single actomyosin rigor bonds: load dependence of lifetime and mechanical properties. *Biophys. J.* **79**, 962–974. (doi:10.1016/S0006-3495(00)76350-8)

Oguchi, Y., Mikhailenko, S. V., Ohki, T., Olivares, A. O., De La Cruz, E. M. & Ishiwata, S. 2008 Load-dependent ADP binding to myosins V and VI: implications for subunit coordination and function. *Proc. Natl Acad. Sci. USA* **105**, 7714–7719. (doi:10.1073/pnas.0800564105)

Oguchi, Y., Mikhailenko, S. V., Ohki, T., Olivares, A. O., De La Cruz, E. M. & Ishiwata, S. 2010 Robust processivity of myosin V under off-axis loads. *Nat. Chem. Biol.* **6**, 300–305. (doi:10.1038/nchembio.322)

Spink, B. J., Sivaramakrishnan, S., Lipfert, J., Doniach, S. & Spudich, J. A. 2008 Long single α-helical tail domains bridge the gap between structure and function of myosin VI. *Nat. Struct. Mol. Biol.* **15**, 591–597. (doi:10.1038/nsmb.1429)

Svoboda, K., Schmidt, C. F., Schnapp, B. J. & Block, S. M. 1993 Direct observation of kinesin stepping by optical trapping interferometry. *Nature* **365**, 721–727. (doi:10.1038/365721a0)

Uchimura, S., Oguchi, Y., Katsuki, M., Usui, T., Osada, H., Nikawa, J., Ishiwata, S. & Muto, E. 2006 Identification of a strong binding site for kinesin on the microtubule using mutant analysis of tubulin. *EMBO J.* **25**, 5932–5941. (doi:10.1038/sj.emboj.7601442)

Uemura, S. & Ishiwata, S. 2003 Loading direction regulates the affinity of ADP for kinesin. *Nat. Struct. Biol.* **10**, 308–311. (doi:10.1038/nsb911)

Uemura, S., Kawaguchi, K., Yajima, J., Edamatsu, M., Toyoshima, Y. Y. & Ishiwata, S. 2002 Kinesin-microtubule binding depends on both nucleotide state and loading direction. *Proc. Natl Acad. Sci. USA* **99**, 5977–5981. (doi:10.1073/pnas.092546199)

Uemura, S., Dorywalska, M., Lee, T. H., Kim, H. D., Puglisi, J. D. & Chu, S. 2007 Peptide bond formation destabilizes Shine–Dalgarno interaction on the ribosome. *Nature* **446**, 454–457. (doi:10.1038/nature05625)

Yanagida, T., Nakase, M., Nishiyama, K. & Oosawa, F. 1984 Direct observation of motion of single F-actin filaments in the presence of myosin. *Nature* **307**, 58–60. (doi:10.1038/307058a0)